4-27-1992

# Fragmentation Clusters Formed in Supercritical Expansions of $^4$He

T. Jiang
*University of Rhode Island*

J. A. Northby
*University of Rhode Island*, jnorthby@uri.edu



Citation/Publisher Attribution

Jiang, T. & Northby, J. A. (1992). Fragmentation clusters formed in supercritical expansions of $^4$He. *Physical Review Letters*, *68*(17), 2620-2623. doi: 10.1103/PhysRevLett.68.2620
Available at: http://dx.doi.org/10.1103/PhysRevLett.68.2620

# Fragmentation Clusters Formed in Supercritical Expansions of $^4$He

T. Jiang and J. A. Northby
*Physics Department, University of Rhode Island, Kingston, Rhode Island 02881*
(Received 23 September 1991)

We have measured the mass distribution of cluster ions formed from a supercritical expansion of helium gas. We find two distinct cluster groups which we identify as condensation and fragmentation clusters. The latter first appear when the expansion conditions approach the critical isentrope. The measurements also suggest that the neutral fragmentation cluster mass distribution is a universal function of the source entropy.

PACS numbers: 67.40.−w, 21.60.−n, 36.40.+d

Helium clusters $He_N$, which are small enough so that a significant fraction of the atoms are in the surface layer (e.g., $N=1$–$10^6$) [1], are especially fascinating objects from two different viewpoints. Since their bound states should be liquidlike they are of considerable theoretical interest as nuclear analogs [2–5]. Also, since they are superfluid for large $N$, it is interesting to ask how this phenomenon will evolve as $N$ decreases through the range where surface effects dominate to its eventual disappearance [1,6,7]. The earliest experimental studies of He cluster beams [8,9] have utilized low-pressure nozzle expansions in which clusters form by condensation of a supersaturated vapor. More recent studies [10–13] have involved high-pressure conditions in which the expansion isentrope passes above the critical point on the phase diagram and enters the coexistence region from the liquid phase. In such "supercritical expansions" clusters should be formed by fragmentation of the liquid jet. To date, no direct measurement of the mass distribution of clusters formed in this process has been made. Indirect evidence suggests that they are fairly large [10] but several puzzling questions remain. For example, in a study of the capture of foreign atoms by He clusters [12] it was found that the effect was largest when the expansion isentrope passed through the critical region. This suggested that such "critical clusters" might be anomalously large compared to those formed under neighboring expansion conditions. The objective of the experiment described here is to measure directly the mass distribution of the charged cluster beam obtained by ionizing clusters formed in a supercritical expansion. For large clusters this should be very similar to the neutral distribution. We utilize a stopping potential energy analysis which is combined with measurements of the beam velocity to yield the mass. This method permits direct measurement of the charged cluster current with an electrometer and, in contrast to other methods which require charge amplifying detectors, leaves no uncertainty associated with an unknown mass-dependent detector sensitivity.

A schematic diagram of the experiment is shown in Fig. 1. Neutral clusters are produced by expanding pure helium gas (99.9999%) from a high-pressure ($P_0=10$–80 bars), low-temperature ($T_0=6$–18 K) stagnation chamber through a 5-$\mu$m sonic nozzle $N$ into an expansion chamber ($P_1<5\times10^{-4}$ torr). After 1.5 cm the beam passes through a 1.0-mm skimmer $S$ into a second differentially pumped chamber ($P_2<5\times10^{-6}$ torr) where it traverses a coaxial electron impact ionizer $I$ located 7 cm behind $S$. We normally use an electron energy $eV_e=35$ eV, which is below the threshold for double ionization by a single electron [11]. The probability of two separate ionizing collisions is small, except for very large clusters, and thus most cluster ions will be singly charged. In normal operation there is no electric field near the beam axis. Thus the velocity of an ionized cluster will be that of its neutral parent, plus any recoil velocity associated with the ionization process. Experiments [13] have indicated that under these conditions recoil effects are small, and consequently we expect the beam to continue largely undeflected. After a further flight path of 43 cm the beam passes through a 1.3-cm collimating aperture into a parallel grid stopping potential energy analyzer $A$. The first grid is held at ground potential, the second carries a variable positive potential $V_s$, and the third (suppressor) grid is normally operated at $V_r=-10$ V to prevent electrons, produced at the Faraday collector $C$ by photons and metastable atoms, from contributing to the current. Stray electrons and background ions produced in the ionizer are prevented from reaching the analyzer by a weak magnetic field ($\approx 10$ G) in the vicinity of the ionizer. The dc collector current $i$ is measured with an electrometer with a sensitivity of about $3\times10^{-15}$ A. We have measured the transmission response of the analyzer with a monoenergetic beam of atomic ions and find that it is sharp to better than 2% of the energy. Within this accuracy, then, the collected current will be

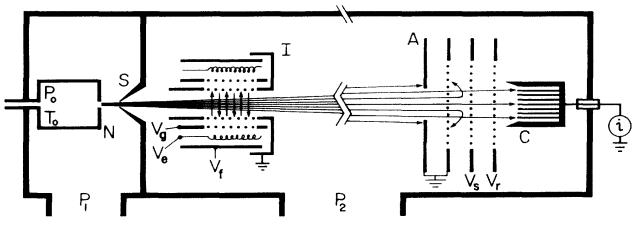


FIG. 1. Schematic of the experiment showing nozzle $N$, skimmer $S$, electron impact ionizer $I$, energy analyzer $A$, and Faraday collector $C$.

proportional to the number of positively charged cluster ions whose energy $E$ exceeds $eV_s$, less any contribution from negatively charged clusters present in the beam. Since the latter contribution, if present, will be insensitive to $V_s$, the energy distribution of the positive-cluster-ion current will be given by $j(E) \propto -di/dV_s$. Furthermore, since the clusters all have the same velocity [14] and thus the same energy per atom, $e_0$, the size distribution of the current is given by $j(N) = e_0 j(E = Ne_0)$.

Typical examples of the dependence of the collector current on the stopping potential are given in Fig. 2. The curves shown are for a range of stagnation temperatures at a fixed pressure, $P_0 = 20.7$ bars. It is obvious that the current is a complex and rapidly varying function of temperature. At 11.0 K we see a small signal from clusters with energies less than 5 eV ($N < 4\times10^3$), which becomes unobservable as the temperature increases. This signal becomes broader and possibly a bit structured at 10.7 K, but at 10.4 K the behavior changes radically. A new and distinct group of clusters with energies greater than 50 eV ($N > 4\times10^4$) appears and rapidly grows in intensity. It is not clear whether the low-energy cluster signal disappears as the temperature decreases, or just becomes unobservable in the presence of the much larger high-energy signal, but there is definitely a range of temperatures in which two distinct cluster groups coexist. The amplitudes of the high- and low-energy components of the signal are smoothly varying and have quite different temperature dependences. Data illustrating this behavior are shown in the inset. Since the low-energy clusters are more divergent than the energetic ones, for these data we have utilized an einzel lens to enhance their contribution to the total current. It is clear that the low-energy cluster signal persists well above the temperature at which the high-energy component has vanished. Thus the existence of two cluster-ion groups cannot be attributed simply to a peculiar ionization-induced fragmentation pattern. Instead it probably reflects a bimodal mass distribution present in the precursor neutral cluster beam. The median energy of the energetic group increases with decreasing temperature from about 70 eV at 10 K ($N \approx 4.2\times10^4$) to 600 eV at 6.5 K ($N \approx 5.5\times10^5$). More detail is provided in Fig. 3, where we show on a logarithmic scale the mass distributions obtained by differentiating the lower-temperature $i$ vs $V_s$ curves. The peak and the low-mass cutoff shift to larger masses as the temperature decreases, and the high-mass distribution decays approximately exponentially, with a rapidly increasing characteristic mass.

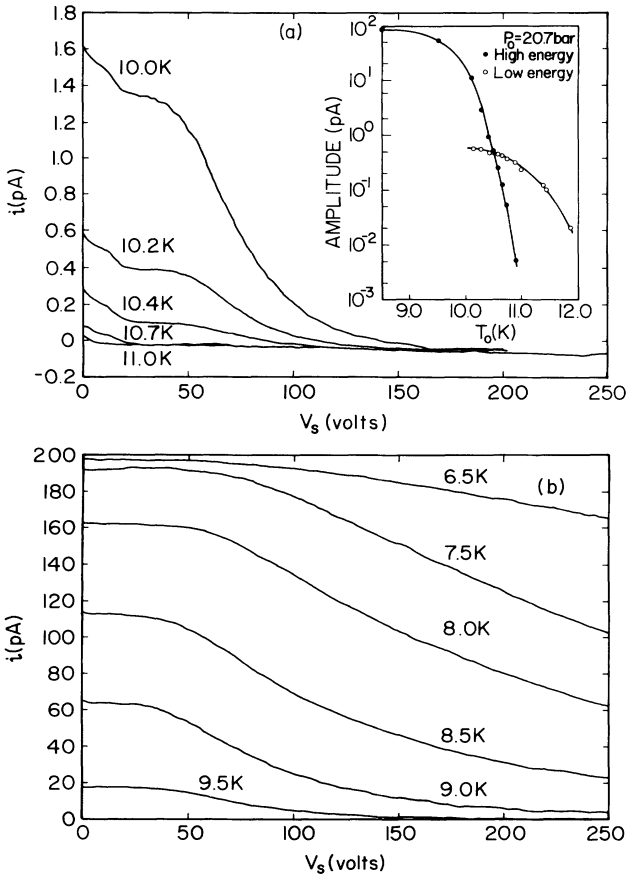


FIG. 2. Collector current $i$ vs stopping potential $V_s$, at source pressure $P_0 = 20.7$ bars and several different source temperatures. (a) $T_0 = 11.0$–$10.0$ K. Inset: The separate temperature dependences of the high- and low-energy signal components when an einzel lens is used to enhance the low-energy signal. (b) $T_0 = 9.5$–$6.5$ K.

As the source pressure is varied the character of the $i(V_s)$ curves remains unchanged. There are still two groups of clusters separated by a region around 30 eV in which there are no clusters. The temperature at which the energetic group first appears changes significantly, however. Arbitrarily defining the threshold to be the temperature $T_0'$ at which the signal at 30 eV, $i(30\ \text{V}) = I^+$, first exceeds 0.1 pA we find that $T_0'$ varies from 10.0 K at $P_0 = 20.7$ bars to 15.4 K at $P_0 = 82.7$ bars.

Nozzle expansions are normally modeled as isenthalpic

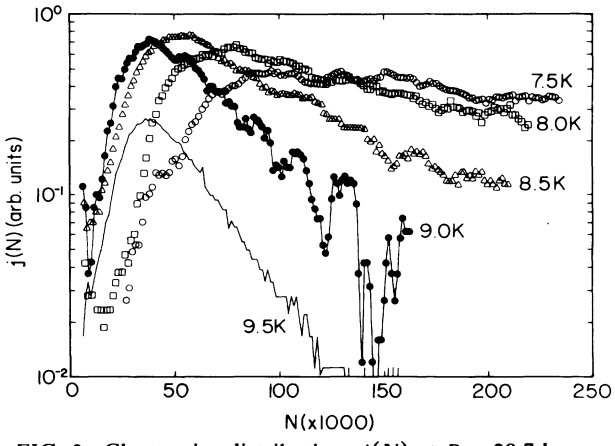


FIG. 3. Cluster size distributions $j(N)$ at $P_0 = 20.7$ bars and source temperatures $T_0 = 9.5$–$7.5$ K.

processes in which the local thermodynamic state follows an isentrope, and it is natural to ask whether the stagnation entropy plays a role here also. It turns out that the thresholds defined above all have the same stagnation entropy [15] $S_0 = 6.4 \pm 0.1$ kJ/kg K. In fact, its role is even more significant as can be seen from Fig. 4, where we show the total large-cluster current $I^+$ for a wide range of $P_0$ and $T_0$ as a function of the single variable $S_0$. (For comparison, we show in the inset the same data plotted as a function of temperature.) To within an amplitude factor of 2 the data are quite closely described by a single universal function of $S_0$. We have indicated the entropy at the critical point in the figure and, for comparison, the liquid and vapor entropies at the lambda point. It is clear that large clusters are present only for expansions which pass through or to the low-entropy side of the critical region. In such supercritical expansions the system enters the metastable (coexistence) region as a superheated liquid and clusters form by fragmentation [10,12]. Normal subcritical expansions produce a supercooled vapor and clusters form by condensation. Consequently, we interpret our large- and small-cluster groups as fragmentation and condensation clusters, respectively. It is not clear why both types coexist in a range of temperatures. It is possible that the state of the system may vary over the beam profile and, since we sample over a finite solid angle, we might see fragmentation near the axis and condensation in the periphery. We have no direct evidence for this, however.

Finally, we note that negative cluster ions [16] may also be present at low intensity in our beam. In order to search for them we have eliminated the positive-ion signal by reducing the ionizing electron energy to $\approx 2$ eV, which is well below the energy needed to produce positive ions. Under these conditions, if we reduce the temperature below a well-defined threshold we are able to generate a fairly intense negative-cluster current $I^-$. This current, as shown in Fig. 4, is again a universal function of $S_0$, but with a significantly lower threshold than for the positive-cluster current. We have also observed [17] that these negative clusters are very energetic ($E > 1000$ eV; $N > 9\times10^5$). Thus negative ions apparently are produced from only the most massive neutral clusters while positive ions come from clusters of all sizes. We can describe formation of both positive- and negative-ion currents $I^+$ and $I^-$ by the single equation

$$I^{\pm} = \int P^{\pm}(N) V_0 \rho(N;P_0,T_0) dN ,$$

where $P^+(N)$ and $P^-(N)$ are the ionization probabilities per unit time in the two cases. $V_0$ is the effective interaction volume and $\rho(N;P_0,T_0)$ is the density of neutral clusters in the ionizer with size $N$ in $dN$. Since $I^+$ and $I^-$ are both universal functions of $S(P_0,T_0)$, and since, for fixed ionizer settings, $P^+(N)$ and $P^-(N)$ are two significantly different functions of the single variable $N$, it is highly likely that $\rho(N;P_0,T_0) = \rho(N;S(P_0,T_0))$ is a universal function of $S_0$ as well [18].

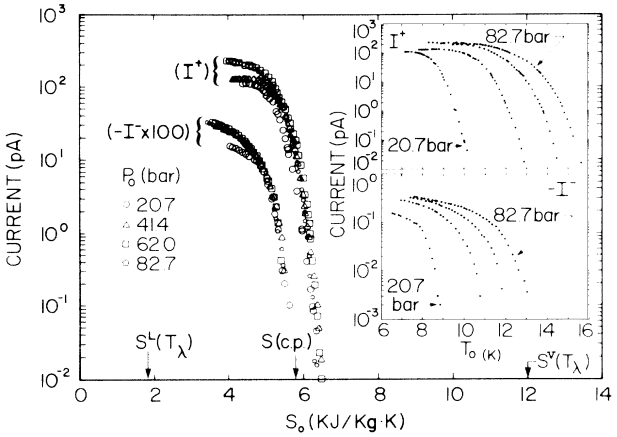


FIG. 4. Positive- and negative-cluster-ion current at four different source pressures as a function of the source entropy. Indicated are the critical point entropy $S$(c.p.) and the liquid and vapor entropies at the lambda point, $S^L(T_\lambda)$ and $S^V(T_\lambda)$. Inset: Ion currents as a function of temperature.

This first direct measurement of the mass distribution of fragmentation cluster ions formed from supercritical expansions has shown that the mean mass is larger and, more importantly, the distribution is much broader than previously supposed [10,13]. These clusters have a very sharp appearance threshold, corresponding closely to expansions along the critical isentrope. While it has been shown [12] that the process of capture, ionization, and ejection of foreign atoms has its maximum intensity for clusters formed under these conditions, the appearance of fragmentation clusters in fact corresponds to the sharp *decrease* in the magnitude of the captured atom signal. Thus it would seem that condensation clusters, while smaller, are nonetheless the most effective for this process. Our experiments also provide strong evidence that the mass distribution of fragmentation clusters is determined solely by the stagnation entropy. In other words, no matter where along an isentrope an expansion starts, the final mass distribution is the same. This could be understood if all expansions along an isentrope reach the same final state, and the resulting fragmentation pattern depends only on that state itself and not on the expansion rate or the fluid velocity when it is reached. The only likely candidates for such well-defined special states along an isentrope are its intersection with the adiabatic spinodal [19,20] and with the $P=0$ isobar, so perhaps a model of fragmentation under these conditions will be required to explain the observed distribution. Recent generalized theories of fragmentation based on the maximum information entropy formalism [21–23] can readily explain a distribution which falls off exponentially with increasing mass, in agreement with our qualitative observations, but it is not easy to explain the cutoff at low masses which we also observe. It is possible that this cutoff is caused by a dynamical effect which takes place after fragmentation,

such as recombination of small and large clusters [24], or by some new conservation principle [21] which applies for adiabatic or zero-pressure fragmentation, but we have found no convincing explanation as yet.

We wish to thank J. P. Toennies for helpful discussions, and S. Y. Sun for help with data acquisition. This work has been supported by the NSF (DMR8816482 and INT8922637).

[1] D. M. Brink and S. Stringari, Z. Phys. D **15**, 257 (1990).
[2] V. R. Pandharipande, S. C. Pieper, and R. B. Wiringa, Phys. Rev. B **34**, 4571 (1986).
[3] *Chemical Physics of Atomic and Molecular Clusters*, Proceedings of the International School of Physics "Enrico Fermi," Course CVII, edited by G. Scoles (North-Holland, Amsterdam, 1990).
[4] S. Stringari and J. Treiner, Phys. Rev. B **36**, 8369 (1987); J. Chem. Phys. **87**, 5021 (1987).
[5] S. A. Chin and E. Krotscheck, Phys. Rev. Lett. **65**, 2658 (1990).
[6] M. V. Rama Krishna and K. B. Whaley, Phys. Rev. Lett. **64**, 1126 (1990); J. Chem. Phys. **93**, 746 (1990); **93**, 6738 (1990).
[7] B. P. Sindzingre, M. L. Klein, and D. M. Ceperly, Phys. Rev. Lett. **63**, 1601 (1989).
[8] J. Gspann, in *Physics of Electronic and Atomic Collisions*, edited by S. Datz (North-Holland, Amsterdam, 1982), p. 79f.
[9] P. W. Stephens and J. G. King, Phys. Rev. Lett. **51**, 1538 (1983).
[10] H. Buchenau, E. L. Knuth, J. A. Northby, J. P. Toennies, and C. Winkler, J. Chem. Phys. **92**, 6875 (1990).
[11] H. Buchenau, J. P. Toennies, and J. A. Northby, J. Chem. Phys. **95**, 8134 (1991).
[12] A. Sheidemann, J. P. Toennies, and J. A. Northby, Phys. Rev. Lett. **64**, 1899 (1990); A. Sheidemann, B. Shilling, J. P. Toennies, and J. A. Northby, Physica (Amsterdam) **165B**, 135 (1990).
[13] K. Martini, J. P. Toennies, and C. Winkler, Chem. Phys. Lett. **178**, 429 (1991); (private communication).
[14] Typical cluster velocities are from 200 to 300 m/s corresponding to energies of 0.8–1.3 meV/atom (Ref. [10]). We have also measured the cluster velocity in our apparatus by synchronous gating of both $V_g$ and $V_s$. Our results are in satisfactory agreement with those of Buchenau *et al.*, and we have used the latter to relate mass and energy in our experiments.
[15] V. V. Sychev, A. A. Vasserman, A. D. Kozlov, G. A. Spiradonov, and V. A. Tysmarny, *Thermodynamic Properties of Helium* (Hemisphere, Washington, 1987).
[16] J. Gspann, Physica (Amsterdam) **169B**, 519 (1991).
[17] Our studies of the negative cluster ions will be reported elsewhere; T. Jiang, S. Sun, and J. A. Northby, in Proceedings of the International Symposium on the Physics and Chemistry of Finite Systems, Richmond, Virginia, 1991 (to be published).
[18] While we do not have detailed $i(V_s)$ data for different pressures at corresponding values of $S_0$, our interpolated results support this hypothesis reasonably well.
[19] A. Vincentini, G. Jacucci, and V. R. Pandharipande, Phys. Rev. C **31**, 1783 (1985).
[20] E. L. Knuth, B. Shilling, and J. P. Toennies, in Proceedings of the Seventeenth International Symposium on Rarefield Gas Dynamics, Aachen, 1990 (to be published).
[21] R. Englman, J. Phys. Condens. Matter **3**, 1019 (1991); R. Englman, N. Rivier, and Z. Yaeger, Philos. Mag. B **56**, 751 (1987).
[22] D. E. Grady and M. E. Kipp, J. Appl. Phys. **58**, 1210 (1985).
[23] B. Holian and D. E. Grady, Phys. Rev. Lett. **60**, 1355 (1988).
[24] F. F. Abraham, S. W. Koch, and R. C. Desai, Phys. Rev. Lett. **49**, 923 (1982).